Fuel 117 (2014) 1231–1241

Contents lists available at ScienceDirect

Fuel

journal homepage: www.elsevier.com/locate/fuel

Gasification performances of raw and torrefied biomass in a downdraft fixed bed gasifier using thermodynamic analysis

Po-Chih Kuo [a], Wei Wu [a,*], Wei-Hsin Chen [b,*]

[a] Department of Chemical Engineering, National Cheng Kung University, Tainan 701, Taiwan, ROC
[b] Department of Aeronautics and Astronautics, National Cheng Kung University, Tainan 701, Taiwan, ROC

HIGHLIGHTS

- Gasification performances of raw and torrefied biomass are thermodynamically analyzed.
- A downdraft fixed bed gasifier is tested using Aspen Plus.
- The modified equivalence ratio and steam supply ratio are considered.
- The cold gas efficiency and carbon conversion are examined.
- The optimum operating conditions for the gasification are found.

ARTICLE INFO

Article history:
Received 11 December 2012
Received in revised form 28 July 2013
Accepted 30 July 2013
Available online 13 August 2013

Keywords:
Biomass gasification
Torrefaction
Syngas
Modified equivalence ratio (ER_m)
Steam supply ratio (SSR)

ABSTRACT

The gasification performances of three biomass materials, including raw bamboo, torrefied bamboo at 250 °C (TB250), and torrefied bamboo at 300 °C (TB300), in a downdraft fixed bed gasifier are evaluated through thermodynamic analysis. Two parameters of modified equivalence ratio (ER_m) and steam supply ratio (SSR) are considered to account for their impacts on biomass gasification. The cold gas efficiency (CGE) and carbon conversion (CC) are adopted as the indicators to examine the gasification performances. The analyses suggest that bamboo undergoing torrefaction is conducive to increasing syngas yield. The higher the torrefaction temperature, the higher the syngas yield, except for TB300 at lower values of ER_m. Because the higher heating value of TB300 is much higher than those of raw bamboo and TB250, the former has the lowest CGE among the three fuels. The values of CC of raw bamboo and TB250 are always larger than 90% within the investigated ranges of ER_m and SSR, but more CO_2 is produced when ER_m increases, thereby reducing CGE. The maximum values of syngas yield and CGE of raw bamboo, TB250, and TB300 are located at (ER_m, SSR) = (0.2, 0.9), (0.22, 0.9), and (0.28, 0.9), respectively. The predictions suggest that TB250 is a more feasible fuel for gasification after simultaneously considering syngas yield, CGE, and CC.

1. Introduction

Gasification is a thermo-chemical conversion technology which transforms solid fuel into gas product through partial oxidation [1]. The main components in the product gas are hydrogen and carbon monoxide and they are called synthesis gas (syngas) [2,3] The generated syngas can be directly consumed as gaseous fuel; it can be further processed to produce electricity and heat. In addition, syngas is a key intermediary in the chemical industry. For example, some liquid transportation fuels, such as methanol, dimethyl ether (DME), and methyl tert-butyl ether (MTBE), can be synthesized from syngas [4–6]. Generally speaking, the quality of syngas varies with the adopted oxidizing agents, such as air, steam, steam–oxygen, air–steam, and oxygen-enriched air [7]. Among these oxidizing agents, air is the most widely employed one [8].

The advantages of air-blown biomass gasification include availability and simplicity, and it has been investigated by numerous researchers using various types of biomass. For instance, Lv et al. [9] studied pine wood block gasification in a downdraft fixed bed gasifier at the equivalence ratios (ERs) of 0.24–0.28; they found that the hydrogen yield and lower heating value (LHV) of syngas were in the ranges of 21.18–29.70 g (kg-biomass)$^{-1}$ and 4.76–5.44 MJ Nm^{-3}. González et al. [10] tested olive orujillo gasification in a laboratory reactor at atmospheric pressure and temperatures of 750–900 °C. They reported that H_2 and CO formation favored high-temperature environments and the maximum H_2 and CO molar fractions occurred at temperatures of 750 and 900 °C, respectively. Gai and Dong [11] demonstrated non-woody

* Corresponding authors. Tel.: +886 6 2757575x62689; fax: +886 6 2344496 (W. Wu), tel.: +886 6 2757575x63600; fax: +886 6 2389940 (W.-H. Chen).
E-mail addresses: weiwu@mail.ncku.edu.tw (W. Wu), weihsinchen@gmail.com (W.-H. Chen).

0016-2361/$ - see front matter © 2013 Elsevier Ltd. All rights reserved.
http://dx.doi.org/10.1016/j.fuel.2013.07.125

Nomenclature

A	total number of atomic masses in the system
AFR	air-to-fuel mass flow rate ratio
SSR	steam supply ratio
a	amount of air per mole of fuel (mol mol fuel^{-1})
a_{ik}	coefficient in element species matrix representing species i containing element k
b	amount of steam per mole of fuel (mol mol fuel^{-1})
CC	carbon conversion (%)
CGE	cold gasification efficiency (%)
c	amount of carbon dioxide per mole of fuel (mol mol fuel^{-1})
d	amount of carbon monoxide per mole of fuel (mol mol fuel^{-1})
ER$_m$	modified equivalence ratio
e	amount of methane per mole of fuel (mol mol fuel^{-1})
f	amount of nitrogen per mole of fuel (mol mol fuel^{-1})
f_i	the fugacity of pure species i
$\hat{f}_i$	the fugacity of species i in solution
G_P	the volume of product gas from the gasification of per unit weight of fuel (Nm^3 kg fuel^{-1})
G^t	total Gibbs free energy of system (J)
G_i^0	a property of pure species i in its standard state (J)
ΔG_f^0	standard Gibbs-energy change of reaction (J mol^{-1})
g	amount of hydrogen per mole of biomass (mol mol fuel^{-1})
$\dot{H}$	the enthalpies of material streams (kJ h^{-1})
HHV	higher heating value fuel (MJ kg fuel^{-1})
L	Lagrange function
LHV$_{\text{product gas}}$	lower heating value of product gas (kJ Nm^{-3})
$\dot{m}$	mass flow rate (kg h^{-1})
N	total number of species in the reaction mixture
n	number of moles
$\dot{Q}_{rxn}$	heat of reaction (kJ h^{-1})
P	pressure (atm)
R	universal gas constant (=8.314 J mol^{-1} K^{-1})
T	temperature (°C)
x	mole fraction
y	mass fraction

Greek letters

μ	chemical potential
ϕ	fugacity coefficient
λ_k	Lagrange multipliers
ω	total number of elements comprising the system

Superscript

^{0}	standard reference state

Subscripts

air	air
ash	ash
biomass	biomass
i	species i
j	species j
k	chemical element index
out	output
rxn	reaction
product gas	product gas of the gasification
steam	steam
x	number of hydrogen atoms per carbon atom in biomass molecule
y	number of oxygen atoms per carbon atom in biomass molecule
z	number of nitrogen atoms per carbon atom in biomass molecule

biomass gasification in a downdraft gasifier at atmospheric pressure. They pointed out that the operating conditions had a significant effect on the gasification efficiency and the gas compositions in the product gas; they also outlined that the optimum value of ER was between 0.28 and 0.32. Nitrogen is contained in the product gas from air-blown gasification; the LHV of the product gas is thus lower and usually in the range of 4–7 MJ Nm^{-3}. In contrast, the LHV of the product gas from gasification using steam as an oxidizer is between 10 and 15 MJ Nm^{-3} and the hydrogen yield is higher [7], as a result of water gas shift reaction. However, biomass steam gasification requires external heat because of the endothermic steam reforming reactions involved [1,12]. By virtue of the aforementioned advantages and disadvantages from air or steam blown process, some studies addressed biomass gasification using the mixture of air and steam as the oxidizing agent [12,13].

In reviewing past literature, in addition to experimental studies, attempts in simulating biomass gasification have been carried out to evaluate the gasification performance affected by various operating conditions. The simulations of biomass gasification can be divided into kinetic rate models and thermodynamic equilibrium models. The equilibrium models are useful tools for recognizing biomass gasification behavior [14]. Li et al. [15] used a non-stoichiometric equilibrium model based on the method of Gibbs free energy minimization to predict the performance of coal gasification. Jarungthammachote and Dutta [16] used the thermodynamic equilibrium model to evaluate the gas compositions in the product gas from the gasification of municipal solid waste in a downdraft gasifier. Nikoo and Mahinpey [17], Doherty et al. [18], and Ramzan et al. [19] adopted the Aspen Plus simulator to predict the compositions and cold gas efficiency (CGE) of the product gas from biomass gasification in a fixed bed, a fluidized bed, and a circulating fluidized bed gasifiers, respectively, where the equilibrium models were adopted as well.

In recent years, torrefied biomass has been widely explored for its feasibility to replace coal [20]. Torrefaction is a mild pyrolysis process carried out at temperatures of 200–300 °C in the absence of oxygen [21,22]. Torrefied biomass is characterized by lower moisture (or hydrophobicity), higher energy density, and improved ignitability, reactivity, and grindability when compared to its parent biomass [23–25]. Because most of the moisture as well as part of the volatiles and hemicellulose in biomass are removed from torrefaction, this pretreatment process produces more uniform feedstocks of consistent quality and makes the control of burning biomass or the use as a feedstock easier. By virtue of these advantages, torrefied biomass is considered as a more valuable fuel than raw biomass.

Most of the studies of biomass gasification were performed using raw biomass as feedstocks and relatively little research has been carried out using torrefied biomass as the fuel in gasification. Prins et al. [26] gave a preliminary assessment of air-blown gasification of torrefied wood and found that the thermodynamic loss was likely to be reduced from torrefied biomass torrefaction. Deng et al. [27] torrefied rice straw and rape stalk for their co-gasification with coal. They mentioned that the properties of the torrefied agricultural residues were closer to those of coal, so torrefaction was a promising method for co-gasification. Couhert et al. [28] evaluated the impact of torrefaction on syngas production from wood gasification in an entrained flow reactor. Seeing that torre-

faction decreased the O/C ratio of the biomass, the quantity of produced syngas increased with the severity of torrefaction.

From the studies of Prins et al. [26], Deng et al. [27], and Couhert et al. [28], it is known that torrefied biomass is a feasible feedstock for biomass gasification or co-gasification. However, just preliminary evaluation of the impact of torrefaction on gasification is provided and there still remains insufficient information in figuring out the gasification performances of torrefied biomass at various operating conditions. The fixed bed gasifiers can be catalogued into three types of reactors; they are updraft, cross-draft, and downdraft fixed bed gasifiers [7]. The updraft fixed bed gasifier is characterized by low exit gas temperature but high tar and ash contents. In the cross-draft fixed bed gasifier, the residence time of produced gas in the high temperature zone is small and this results in the significant amount of tar in the outgoing gas. With regard to the downdraft fixed bed gasifier, the gas temperature at the exit is high, while tar and ash contents are low. It follows that the gasification behavior in a downdraft gasifier is closer to the thermodynamic equilibrium. For this reason, the purpose of this study is to explore biomass gasification in a downdraft fixed bed gasifier via a thermodynamic equilibrium model. The gasification performances of raw and torrefied biomass will be compared with each other. The parameters of modified equivalence ratio (ERm) and steam supply ratio (SSR) are considered to account for their influences on gasification performances, such as syngas yield, cold gas efficiency, and carbon conversion. The optimum operation of biomass gasification will also be outlined.

2. Methodology

2.1. Assumptions

The following assumptions are employed to simplify the simulations of biomass gasification.

(1) Biomass gasification processes are isothermal and in steady state.
(2) The gasifier is operated at the thermodynamic equilibrium state; that is, the residence time of reactants is sufficiently long so that the reactions in the reactor are in chemical equilibrium.
(3) The feedstock is at normal conditions (i.e. 25 °C and 1 atm).
(4) The product gas is a mixture of H_2O, N_2, H_2, CO, CO_2, and CH_4, and all the gases follow the ideal gas law.
(5) The sulfur content in the feedstocks and the formation of air pollutants, such as COS, H_2S, CS_2, NH_3, and HCN, are neglected.
(6) Char contains solid carbon (C) and ash alone, and tar formation is disregarded.

2.2. Gasification model

The gasification model in this study is based on Gibbs free energy minimization method [16,29]. The total Gibbs free energy (G^t) is a function of temperature, pressure, and number of moles of species i(n_i), so it is given by

$$(G^t)_{T,P} = g(n_1, n_2, n_3, \cdots, n_i) \tag{1}$$

In a system at thermodynamic equilibrium, the total Gibbs free energy is defined as

$$G^t = \sum_{i=1}^{N} n_i \mu_i \tag{2}$$

In the preceding equation, μ_i is the chemical potential of species i and it is presented by

$$\mu_i = G_i^0 + RT \ln\left(\hat{f}_i / f_i^0\right) \tag{3}$$

where $\hat{f}_i$, G_i^0, and f_i^0 are the fugacity of species i in the gas mixture, the standard Gibbs free energy, and the standard fugacity of species i, respectively. For a fluid following the ideal gas law at the standard state (i.e. 1 atm), $f_i^0 = P^0$. Eq. (3) is thus presented in terms of pressure as

$$\mu_i = G_i^0 + RT \ln\left(\hat{f}_i / P^0\right) \tag{4}$$

G_i^0 is equal to zero for each chemical element at standard state, hence $G_i^0 = \Delta G_{f_i}^0$ for each component where $\Delta G_{f_i}^0$ is the standard Gibbs free energy of formation of species i at 1 atm. For the gas phase reactions, $\hat{f}_i = y_i \hat{\varphi}_i P$. Accordingly, Eq. (4) becomes

$$\mu_i = \Delta G_{f_i}^0 + RT \ln(y_i \hat{\varphi}_i P / P^\circ) \tag{5}$$

If all gases are assumed as the ideal gases at one atmospheic pressure, substituting Eq. (5) into Eq. (2) gives

$$G^t = \sum_{i=1}^{N} n_i \Delta G_{f_i}^0 + \sum_{i=1}^{N} RT \ln(y_i) \tag{6}$$

To find the values of n_i which minimize the objective function G^t, they are subject to the constraints of material mass balance. The minimization of the Gibbs free energy can be solved by introducing the Lagrange's undetermined multipliers as [30]:

$$\sum_{i=1}^{N} n_i a_{ik} = A_k (k = 1, 2 \cdots, \omega) \tag{7}$$

where a_{ik} and A_k are the numbers of atoms of k element in each molecule of species i and the total number of atoms of k element in the system, respectively, and ω is the total number of elements comprising the system. Then the Lagrange multipliers λ_k is introduced by multiplying it into each equation of material mass balance as

$$\lambda_k \left(\sum_{i=1}^{N} n_i a_{ik} - A_k \right) = 0 \quad (k = 1, 2 \cdots, \omega) \tag{8}$$

The summation of the equations over k gives

$$\sum_k \lambda_k \left(\sum_{i=1}^{N} n_i a_{ik} - A_k \right) = 0 \tag{9}$$

A Lagrange function L is formed when this summation is added into G^t and it is expressed as

$$L = G^t + \sum_k \lambda_k \left(\sum_{i=1}^{N} n_i a_{ik} - A_k \right) \tag{10}$$

The minimization of L takes place when its partial derivatives are all equal to zero. Therefore, the system reaches the equilibrium state when the partial derivatives of Eq. (10) are equal to zero, that is

$$\left(\frac{\partial L}{\partial n_i} \right)_{T,P,n_j} = 0 \quad (i = 1, 2, \cdots, N, \ \text{and} \ i \neq j) \tag{11}$$

2.3. Mass and energy balances

Four elements of carbon, hydrogen, oxygen, and nitrogen are the major components in biomass; hence the feedstocks are expressed by $CH_xO_yN_z$ where the subscripts x, y, and z are determined

from the elemental analysis of biomass. Based on the mass balance, the global gasification reaction is written as

$$CH_xO_yN_z + a(O_2 + 3.76\ N_2) + bH_2O \rightarrow cCO_2 + dCO + eCH_4 + fN_2 + gH_2 \quad (12)$$

where a is the amount of air per mol of biomass and b is the amount of supplied steam; c, d, e, f, and g are the numbers of moles of CO_2, CO, CH_4, N_2, and H_2, respectively.

The energy balance between the reactants and the products is calculated based on the following equations

$$\sum_{in}\dot{H}_i + \dot{Q}_{rxn} = \sum_{out}\dot{H}_j \quad (13)$$

$$\sum_{in}\dot{H}_i + \dot{Q}_{rxn} = \dot{H}_{biomass} + \dot{H}_{air} + \dot{H}_{steam} \quad (14)$$

$$\sum_{out}\dot{H}_j = \dot{H}_{product\ gas} + \dot{H}_{ash} + \dot{H}_{steam} \quad (15)$$

where $\sum_{in}\dot{H}_i$ and $\sum_{out}\dot{H}_j$ are the enthalpy rates of input and output material streams, respectively. All inputs on the left-hand side of Eq. (13) are at 25 °C and outputs on the right-hand side are at the gasification temperature. $\dot{H}_{biomass}, \dot{H}_{steam}, \dot{H}_{product\ gas}$, and $\dot{H}_{ash}$ are the rates of heat of formation of biomass, steam, gaseous products, and ash, respectively, and $\dot{Q}_{rxn}$ is the rate of heat of reaction.

The impacts of two operating parameters of modified equivalence ratio (ER_m) and steam supply ratio (SSR) on biomass gasification are taken into account [7,12]. Different from the study of Gordillo et al. [12], the modified equivalence ratio (ER_m) is defined as the ratio of the total actual oxygen mass supplied by both air and steam to the stoichiometric oxygen. SSR accounts for the oxygen supply ratio from steam and from both air and steam. The parameters of ER_m and SSR are expressed as

$$ER_m = \frac{\dot{m}_{oxygen\ in\ air} + \dot{m}_{oxygen\ in\ steam}}{\dot{m}_{oxygen\ in\ stoichiometry}} \quad (16)$$

$$SSR = \frac{\dot{m}_{oxygen\ in\ steam}}{\dot{m}_{oxygen\ in\ air} + \dot{m}_{oxygen\ in\ steam}} \quad (17)$$

For a given ER_m, a higher SSR means a higher steam supply to replace air supply for oxidizing agent.

2.4. Stream and thermodynamic properties

The present study employed Aspen Plus V7.3 to evaluate biomass gasification. The information of property models and parameters are listed in Table 1. The stream classes were used to define the structure of simulation streams. The components of biomass and ash are not available in the standard Aspen Plus component database. Hence, the MCINCPSD stream class, which contains three substreams comprising MIXED, CIPSD, and NCPSD, was used in this simulation. Aspen Plus can apply various equations of state to study phase behavior of pure compounds and multi-component mixtures over wide ranges of temperature and pressure. In this study, Peng–Robinson equation of state was utilized to estimate the physical properties. The HCOALGEN model included a number of empirical correlations for heat of combustion, heat of formation, and heat capacity, hence the enthalpies of nonconventional components, say, biomass and ash, were calculated by the model. The density of biomass was evaluated by DCOALIGT model [19].

Table 1
Simulation of operating condition and gasification parameters.

Items	Parameters	
Stream class	MCINCPSD	
Thermodynamic property	Peng–Robinson	
Nonconventional properties	Enthalpy	HCOALGEN
	Density	DCOALIGT
Feedstock	Raw bamboo	$CH_{1.39}O_{0.34}N_{0.009}$
	Torrefied bamboo (250 °C)	$CH_{1.18}O_{0.24}N_{0.008}$
	Torrefied bamboo (300 °C)	$CH_{0.82}O_{0.13}N_{0.001}$
Ambient conditions	25 °C and 1 atm	
Input conditions	Fuel:	25 °C and 1 atm
	Air:	25 °C and 1 atm
	Steam:	200 °C and 1 atm
Gasifier	900 °C and 1 atm	
Sensitivity analysis	ER_m	0.2–0.4
	SSR	0–0.9

2.5. System description

Typically, the gasification processes are partitioned into the following reactions zones [7,10,11].Drying zone

$$H_2O_{(l)} \rightarrow H_2O_{(g)}, \quad q\Delta H^0 = +40.7\ kJ\ mol^{-1} \quad (18)$$

Devolatilization zone

$$CH_xO_yN_z \rightarrow char + volatiles \quad (19)$$

Oxidation zone

$$C + 0.5O_2 \rightarrow CO, \quad \Delta H^0 = -268\ kJ\ mol^{-1} \quad (20)$$

$$C + O_2 \rightarrow CO_2, \Delta H^0 = -406\ kJ\ mol^{-1} \quad (21)$$

Reduction zoneWater gas reaction

$$C + H_2O \rightarrow CO + H_2, \quad \Delta H^0 = +131.4\ kJ\ mol^{-1} \quad (22)$$

Boudouard reaction

$$C + CO_2 \rightarrow 2CO, \Delta H^0 = +172.6\ kJ\ mol^{-1} \quad (23)$$

Shift reaction

$$CO + H_2O \leftrightarrow CO_2 + H_2, \Delta H^0 = -42\ kJ\ mol^{-1} \quad (24)$$

Methanation reaction

$$C + 2H_2 \leftrightarrow CH_4, \Delta H^0 = -75\ kJ\ mol^{-1} \quad (25)$$

For the purpose of analysis, the reaction zones are represented by a number of blocks. Fig. 1 shows the flow chart of biomass gasification simulation using Aspen Plus and Table 2 gives the brief descriptions of the unit operations of the blocks. The stream BIOMSS was specified as a nonconventional stream and it was defined in terms of proximate and elemental analyses. When BIOMASS was fed into the system, the first step was the heating and drying of biomass. The blocks DRYER and DRYFLASH were used to model the drying process, and the moisture in the feedstock was removed from EXHUAST stream, as shown in Fig. 1. After drying, the devolatilization stage was performed in the block DECOMP in which the RYield reactor was used. In DECOMP, the feedstock was transformed from a non-conventional solid into volatiles and char. The volatiles consisted of carbon, hydrogen, oxygen, and nitrogen, and the char was converted into ash and carbon, based on the ultimate analysis [17–19]. The yield of volatiles was equal to the volatile content in the fuel according to the proximate analysis. Moreover, the actual yield distributions in DECOMP were calculated by a calculator block which was controlled by FORTRAN statement in accordance with the component characteristics of the feedstock. The combustion and gasification of biomass were simulated by a block called GASIFIER in which the chemical equilibrium was determined by minimizing the Gibbs free energy. The product stream was then cooled to room temperature by COOLER. Water was heated in the block HEATER to become steam named STEAM;

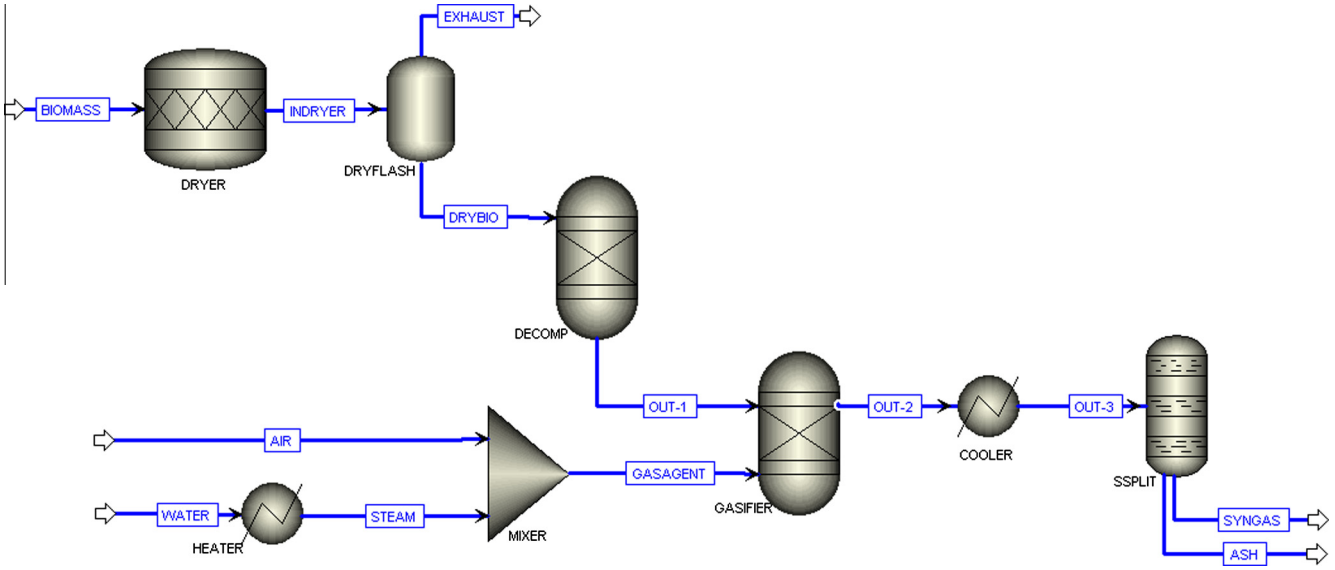

Fig. 1. Flow chart of biomass gasification simulation using Aspen Plus.

Table 2
Description of the unit operations of the blocks in the flow char of Fig. 1.

Aspen Plus name	Block name	Description of function
RStoic	DRYER	Drying of fuel
Flash2	DRYFLASH	Calculation of vapor–liquid equilibrium
RYield	DECOMP	Decomposition of fuel according to its proximate and ultimate analyses
RGibbs	GASIFER	Gasification and combustion of fuel
Heater	HEATER	Heat supplied for steam generation
	COOLER	Cooling of product gas
SSplit	SSPLIT	Separation of inert ash from product gas
Mixer	MIXER	Blending of air and steam into one stream

the streams AIR and STEAM were blended in MIXER and the mixture was utilized as the oxidizing agent. Eventually, the product gas was divided into two streams SYNGAS and ASH in the block SSPLIT.

2.6. Model validation

In the present simulations, the RGibbs reactor (Table 2) was utilized to predict the equilibrium composition of the produced gas, and the predictions were based on the Gibbs energy minimization method. To ensure the developed model in the present study is purely an equilibrium model, the obtained values of CO conversion from water gas shift reaction at various steam/CO ratios and reaction temperatures are compared with the thermodynamic analyses of Chen et al. [31]. In Fig. 2, the predictions from the RGibbs reactor in Aspen Plus are in good agreement with the results of Chen et al. [31]. This verifies that the adopted model in this study is purely an equilibrium model. The thermodynamic model of gasification is also validated by comparing the current predictions to the experimental results of Jayah et al. [32]. In their experiments, rubber wood was fed into a downdraft fixed bed gasifier operated at atmospheric pressure (1 atm) along with the gasification temperature of 900 °C. Three different air-to-fuel mass flow rate ratios (AFRs) of 2.03, 2.20, and 2.37 are considered for comparison and the comparisons of H_2, CO, CO_2, and CH_4 concentrations are displayed in Fig. 3. The maximum relative errors of H_2, CO and CO_2 concentrations between the thermodynamic analyses and experimental measurements are 8.37%, 7.89%, and 7.14%, respectively, revealing that the predicted results of the three gases at various AFRs agree with the experimental measurements (Fig. 3a–c). The experimental values of CH_4 concentration are in the range of 1.1–1.4%, whereas the predictions are close to zero (Fig. 3d). Similar results were also observed in the study of Jarungthammachote and Dutta [33] and Baratieri et al. [34]. The measured CH_4 concentration cannot be explained based on a purely thermodynamic equilibrium because of incomplete conversion of pyrolysis products [34]. Because CH_4 is not the main species in the product gas, the above comparison reveals that the developed thermodynamic model is reliable in the present work.

3. Results and discussion

In this study, three kinds of biomass [35] are selected as the feedstocks to be investigated; they are bamboo, torrefied bamboo at 250 °C (TB250), and torrefied bamboo at 300 °C (TB300). The bamboo was individually torrefied at 250 and 300 °C for one hour. The properties of the feedstocks, such as the proximate analysis, elemental analysis, and higher heating values (HHV) are listed in Table 3. The biomass gasification is fulfilled in a downdraft fixed bed gasifier at 900 °C and 1 atm. Details of the operating conditions are given in Table 1.

3.1. Effect of ER_m

The supply of oxidizing agent, namely, ER_m, plays an important role in the performance of biomass gasification. A low ER_m will lead to biomass reactions approaching pyrolysis, whereas a high ER causes biomass combustion. After testing, the appropriate ER_m for biomass gasification is in the range of 0.2–0.4; hence the aforementioned range of ER_m serves as the basis of the present study. Table 4 displays the dry-basis concentrations of H_2, CO, and CO_2 from biomass gasification at the condition of SSR = 0 (i.e. no steam is supplied as the oxidizer). The H_2 concentration decreases with increasing ER_m, regardless of which biomass is used as the feedstock. Similar to H_2 formation, the CO concentration also decreases with increasing ER_m but an opposite trend in CO_2 concentration is exhibited. This can be explained by more oxygen supplied for biomass reactions which have a trend toward fuel combustion when ER_m rises. The gasification of raw bamboo produces the highest H_2 concentration among the three fuels, whereas TB300 gives the

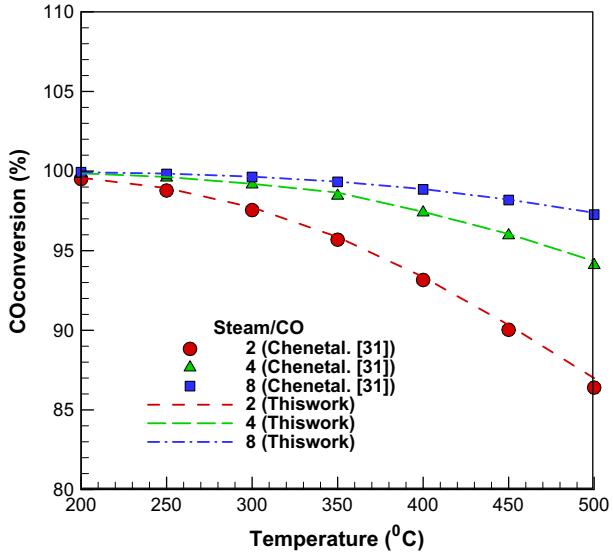

Fig. 2. Comparisons of CO conversion from water gas shift reaction at various steam/CO ratios and reaction temperature.

lowest H_2 concentration. It has been reported that the moisture content in feedstock affected the gas compositions of product gas [32] and a higher moisture content in the feedstock led to a higher H_2 concentration in the product gas [16]. By virtue of higher moisture content in raw bamboo (Table 3), its gasification results in the higher H_2 concentration compared to the gasification of the others.

Table 3
Proximate and elemental analyses of three feedstocks used in simulations [35].

Feedstock	Raw bamboo	TB250	TB300
Proximate analysis (wt%)			
Moisture	5.76	3.32	2.97
Volatile matter (VM)	78.76	70.20	48.05
Fixed carbon (FC)	14.4	25.05	47.03
Ash	1.08	1.43	1.95
Elemental analysis (wt%)			
C	48.64	56.58	69.56
H	5.64	5.55	4.77
N	0.52	0.52	0.12
O	44.09	35.9	23.6
S	0.03	0.02	0
Higher heating value (MJ kg^{-1})			
	18.94	20.99	27.23

Conversely, the gasification of raw bamboo gives the lowest CO concentration among the three materials, stemming from its lowest carbon content. Torrefaction is able to reduce the atomic H/C and O/C ratios of biomass to a certain extent [20,21]. For the gasification of TB300, the variation of CO and CO_2 concentrations is insensitive to ER_m when it increases from 0.2 to 0.26. This may be due to relatively more carbon being contained in TB300 (Table 3). However, the flow rates of CO and CO_2 at the exit of the gasifier increases with increasing ER_m. Within the aforementioned range of ER_m, the lower H_2 concentration from the gasification of TB300 than from raw bamboo and TB250 is possibly attributed to the lower moisture content in the former.

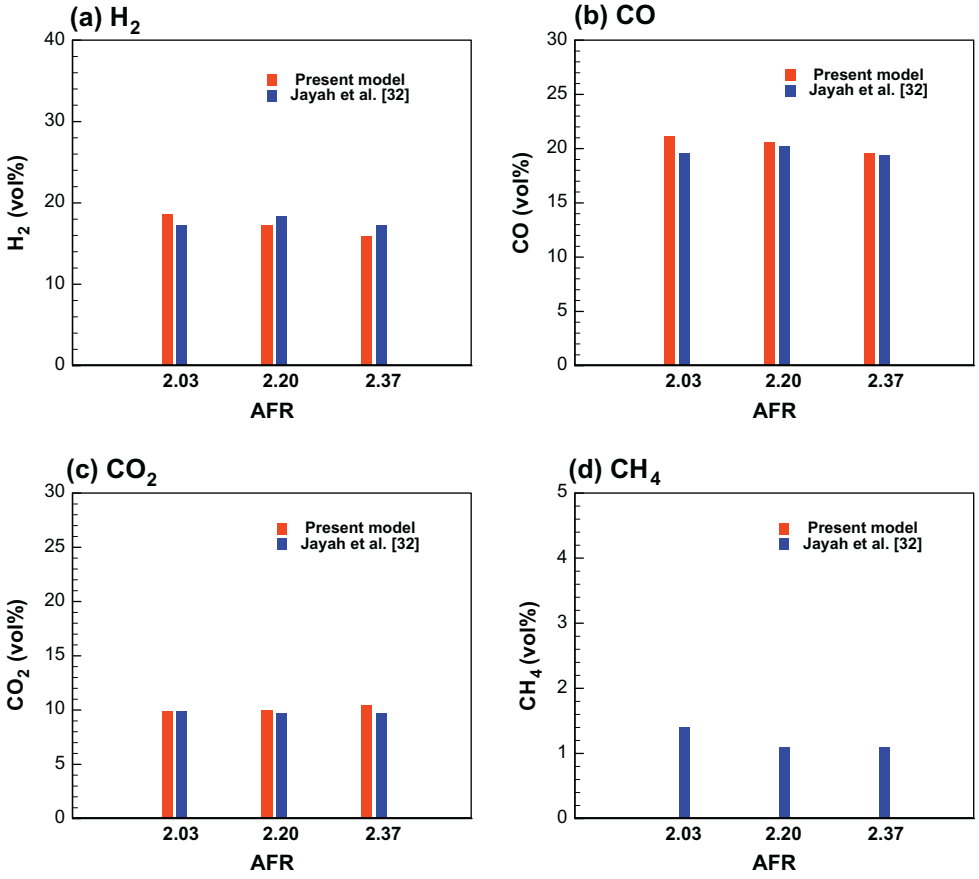

Fig. 3. Comparisons of (a) H_2, (b) CO, (c) CO_2, and (d) CH_4 concentrations between thermodynamic predictions and experimental measurements.

Table 4
Gas concentrations in the product gases from the gasification of raw bamboo, TB250, and TB300 (vol%, dry basis).

ER_m	Raw bamboo			TB250			TB300		
	H_2	CO	CO_2	H_2	CO	CO_2	H_2	CO	CO_2
0.2	29.23	35.75	3.30	27.22	38.22	0.46	23.34	35.79	0.41
0.22	27.75	34.13	4.04	25.91	36.83	1.09	22.00	35.69	0.41
0.24	26.34	32.58	4.75	24.53	35.06	1.96	20.80	35.60	0.40
0.26	24.99	31.08	5.43	23.20	33.36	2.79	19.73	35.52	0.40
0.28	23.71	29.64	6.09	21.93	31.73	3.60	18.72	34.76	0.77
0.3	22.47	28.26	6.73	20.71	30.16	4.37	17.61	32.89	1.75
0.32	21.30	26.93	7.35	19.55	28.65	5.11	16.53	31.10	2.70
0.34	20.17	25.64	7.94	18.45	27.21	5.83	15.50	29.39	3.60
0.36	19.09	24.40	8.51	17.39	25.81	6.52	14.52	27.75	4.47
0.38	18.05	23.21	9.07	16.38	24.47	7.19	13.59	26.17	5.31
0.4	17.06	22.06	9.61	15.42	23.18	7.83	12.71	24.66	6.11

In examining the distributions of syngas yield, Fig. 4a depicts that the syngas yield is lifted when bamboo is torrefied. The syngas yield from the gasification of TB250 is higher than that of raw bamboo by approximately 15–17%; the gasification of TB300 further increases the syngas yield by factors of 30–37% when ER_m is no less than 0.26. Seeing that more carbon is in TB300 and insufficient oxygen is supplied at ER_m = 0.20, its syngas yield is even lower than that of TB250. This results in that the maximum syngas yield develops at ER_m = 0.28. The lower heating value (LHV) of product gas is expressed as [13]

$$\mathrm{LHV_{product\ gas}(kJ\ Nm^{-3})} = \left(30.0x_{CO} + 25.7x_{H_2} + 85.4x_{CH_4}\right) \times 4.2 \quad (26)$$

where x stands for the mole fraction of gas species in the product gas (dry basis). As a whole, the LHV of the product gas shown in Fig. 4b depends strongly on ER_m and it is in the range of 4.49 and 7.81 MJ Nm^{-3}. On the other hand, the influence of feedstock on LHV is slight. Using torrefied bamboo as the feedstock lowers the H_2 concentration in the product gas (Table 4), whereas it promotes the CO concentration. The former intensifies the LHV of the product gas but the latter abates it. This is the reason that the three curves shown in Fig. 4b are close to each other. In summary, more syngas is produced when torrefied bamboo is used as the feedstock, but the energy content of the product gas per unit volume changes slightly. When the two factors are considered together, as a result, the total energy of the product gas from the gasification of torrefied biomass goes up.

3.2. Cold gas efficiency and carbon conversion

The cold gas efficiency (CGE) is a crucial index to account for the performance of biomass gasification and it is defined as [11]

$$\mathrm{CGE}(\%) = \frac{G_P \times \mathrm{LHV_{product\ gas}}}{\mathrm{HHV_{fuel}}} \times 100 \quad (27)$$

where G_P is the volume of product gas from the gasification of per unit weight of fuel (Nm^3 kg $fuel^{-1}$) and HHV_{fuel} is the higher heating value of fuel (MJ kg $fuel^{-1}$), respectively. Fig. 5a suggests that increasing ER_m lessens the value of CGE, stemming from the reduction of syngas yield (Fig. 4a). For the three fuels, the value of CGE is below 50% as long as ER_m is larger than 0.28. It follows that ER_m should be controlled below 0.3 from the thermodynamic point of view. When raw bamboo is torrefied at 250 and 300 °C, their HHV values are amplified by factors of 10.8% and 43.8%, respectively (Table 3). The increase in the HHV of TB300 results in its CGE being lower than the other two fuels as indicated in Eq. (27), even though the syngas yield is lifted.

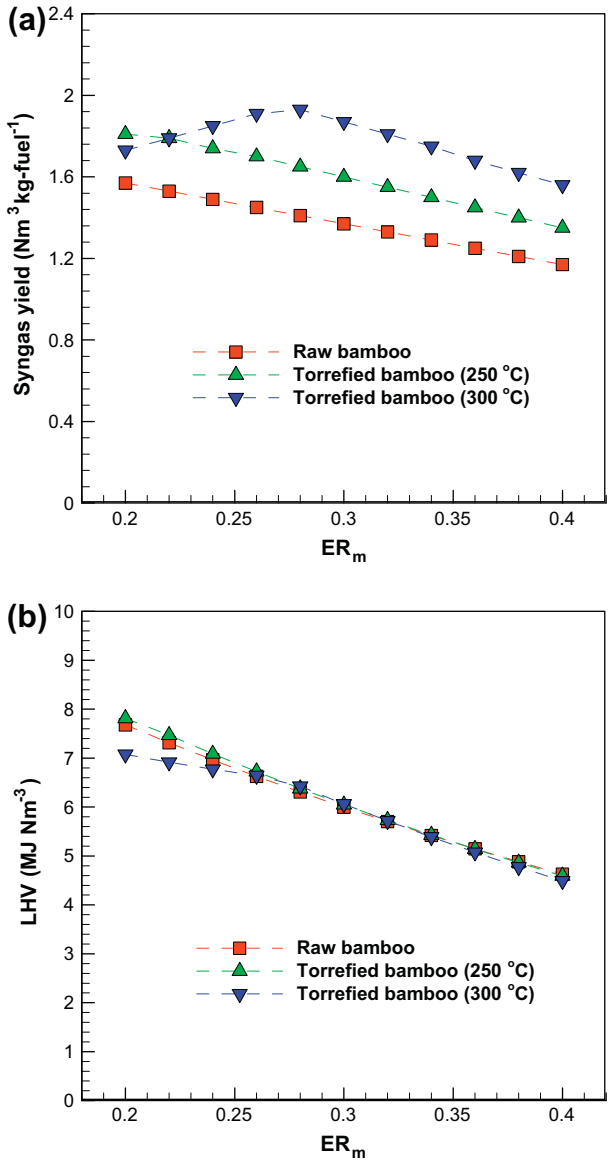

Fig. 4. Distributions of (a) syngas yield and (b) lower heating value from the gasification of three fuels (SSR = 0).

In addition to CGE, the carbon conversion (CC) of the gasification system is also analyzed and it is defined as

$$\mathrm{CC}(\%) = \left(1 - \frac{\dot{m}_{\mathrm{product\ gas}}\left(y_{CO_2}\frac{12}{44} + y_{CO}\frac{12}{28} + y_{CH_4}\frac{12}{16}\right)}{\dot{m}_{\mathrm{fuel}}y_c}\right) \times 100 \quad (28)$$

where y_i is the mass fraction of species i in the product gas. The concentration of CH_4 in the product gas is fairly low, implying that most of the carbon in feedstock is converted into CO and CO_2. For raw bamboo and TB250, over 92% of carbon in the feedstocks is consumed, as shown in Fig. 5b. The CC of raw bamboo is slightly higher than that of TB250. In regard to TB300, it is not surprised that its CC is lower than those of the others, as a consequence of lower CGE, especially at ER_m < 0.28 (Fig. 5a). When ER_m is larger than or equal to 0.28, the CC of TB300 is around 90.6%. Though more carbon is converted at higher values of ER_m, more CO_2 and less CO are produced (Table 4). The value of CGE decreases rather than increases with increasing ER_m.

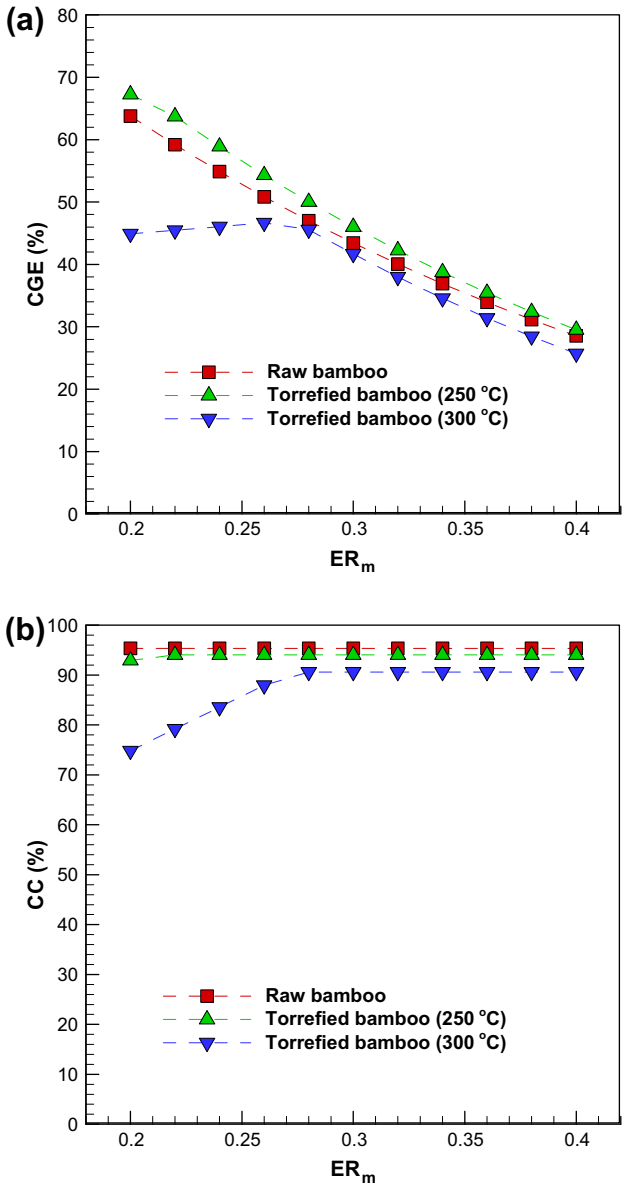

Fig. 5. Distributions of (a) cold gas efficiency and (b) carbon conversion from the gasification of three fuels (SSR = 0).

Table 5
Optimum operating conditions of three fuels (SSR = 0).

Material	Raw	TB250	Increasing factor[a] (%)	TB300	Increasing factor[a] (%)
Optimum ER_m	0.20	0.20	–	0.27	–
Syngas yield (Nm^3/kg)	1.57	1.81	15.29	1.95	24.20
LHV (MJ/Nm^3)	7.68	7.81	1.69	6.57	−14.45
CGE (%)	63.79	67.26	5.44	47.08	−26.20
CC (%)	95.37	92.93	−2.56	90.63	−4.97

[a] Increasing factor $= \frac{\text{Torrefied bamboo} - \text{Raw bamboo}}{\text{Raw bamboo}} \times 100$.

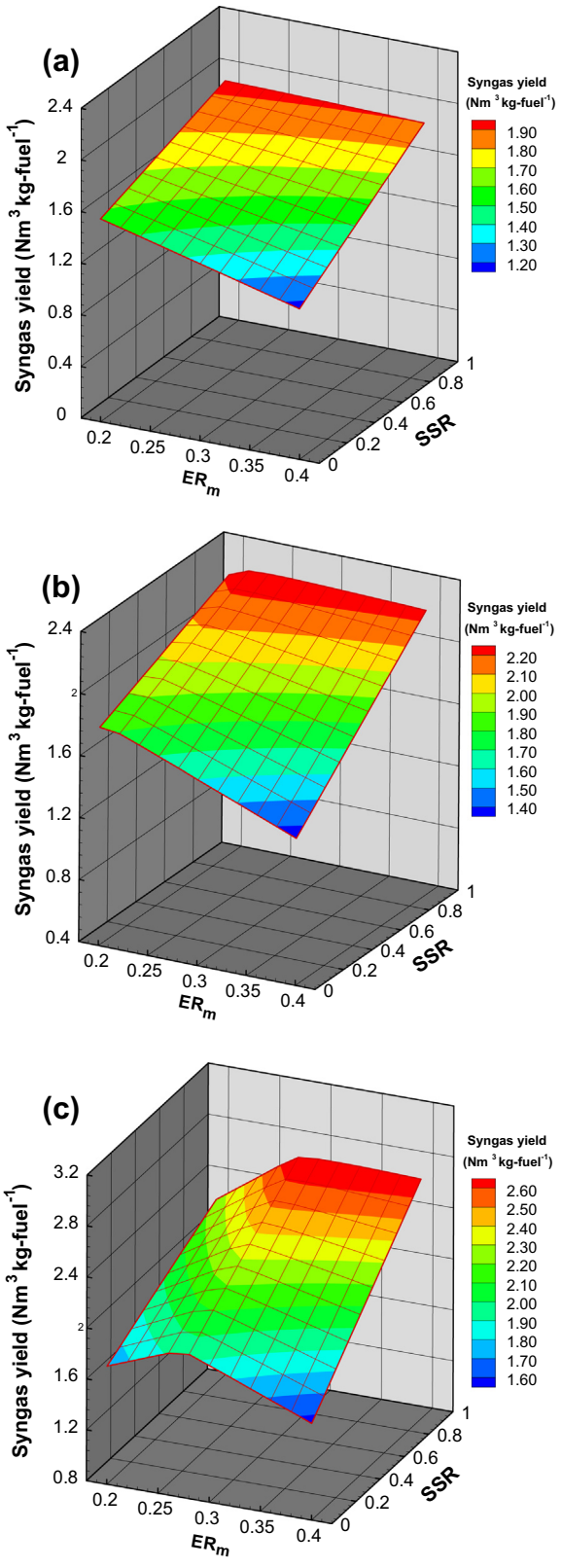

Fig. 6. Three-dimensional distributions of syngas yield from the gasification of (a) raw bamboo, (b) torrefied bamboo at 250 °C and (c) torrefied bamboo at 300 °C.

From the above observations, the optimum operating conditions and the gasification results of the three fuels at SSR = 0 are summarized in Table 5. For the raw bamboo and TB250, they should be operated at $ER_m = 0.2$. A comparison between the two fuels, Table 4 indicates that the syngas yield is increased by a factor of 15.29% if the bamboo is torrefied at 250 °C for 1 h. However, the increment in the LHV and CGE of the product gas is relatively slight. The CC of TB250 is even lower than that of raw bamboo. For TB300, the optimum operation is located at $ER_m = 0.272$ and its syngas yield is higher than that of raw bamboo by 24.2%. However, the values of LHV, CGE, and CC of TB300 are lower than those

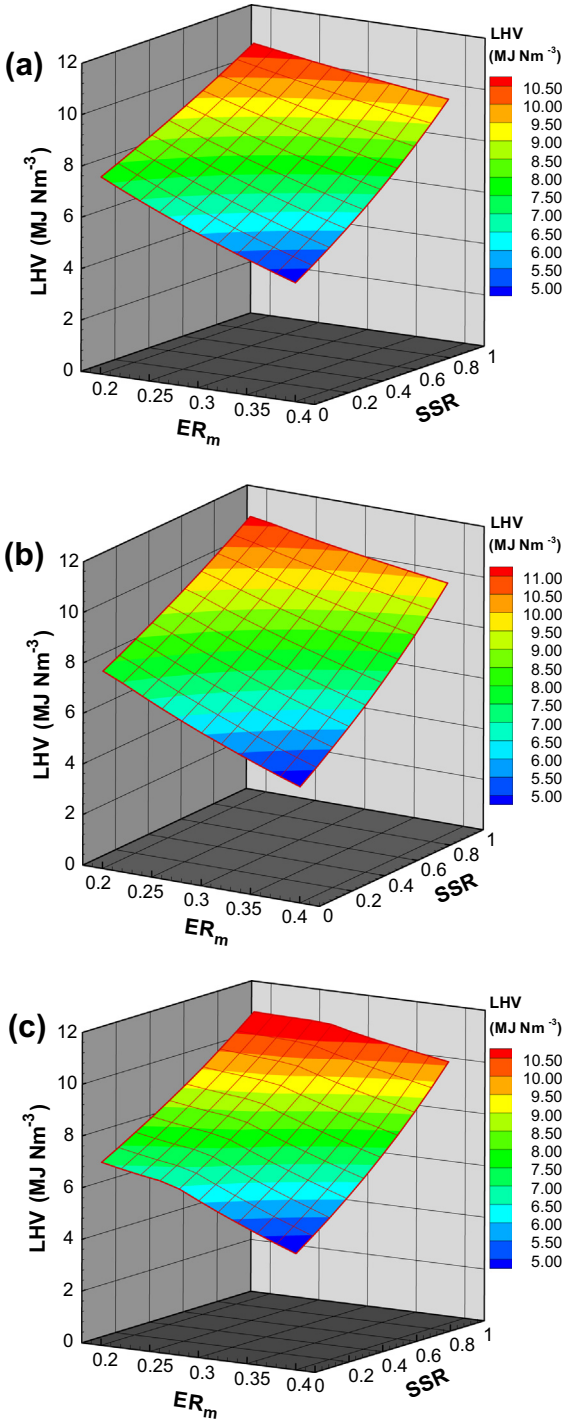

Fig. 7. Three-dimensional distributions of lower heating value from the gasification of (a) raw bamboo, (b) torrefied bamboo at 250 °C and (c) torrefied bamboo at 300 °C.

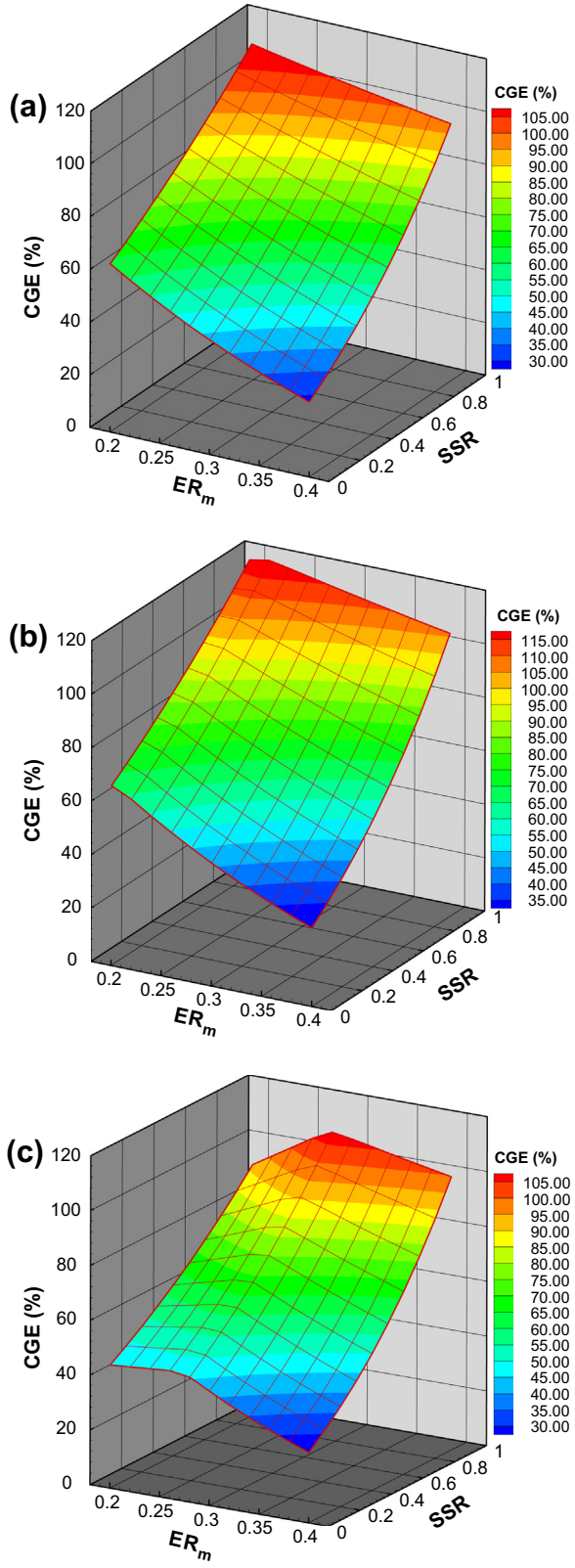

Fig. 8. Three-dimensional distributions of cold gas efficiency from the gasification of (a) raw bamboo, (b) torrefied bamboo at 250 °C and (c) torrefied bamboo at 300 °C.

of raw bamboo and TB250. Accordingly, from the practical point of view, TB250 is a better feedstock for fuel gasification and syngas production.

3.3. Effect of steam

Subsequently, attention is paid to the effect of steam on the gasification results. The three-dimensional profiles of syngas yield, LHV, CGE, and CC are plotted in Figs. 6–9, respectively, where SSR ranges from 0 to 0.9. At present, 11 different values of ER_m (i.e. 0.2, 0.22, 0.24, 0.26, 0.28, 0.30, 0.32, 0.34, 0.36, 0.38, and 0.40) and 10 different values of SSR (i.e. 0, 0.1, 0.2, 0.3, 0.4, 0.5, 0.6, 0.7, 0.8, and 0.9) are taken into account. It is impossible to list all the operating conditions in a table. Therefore, only the air and

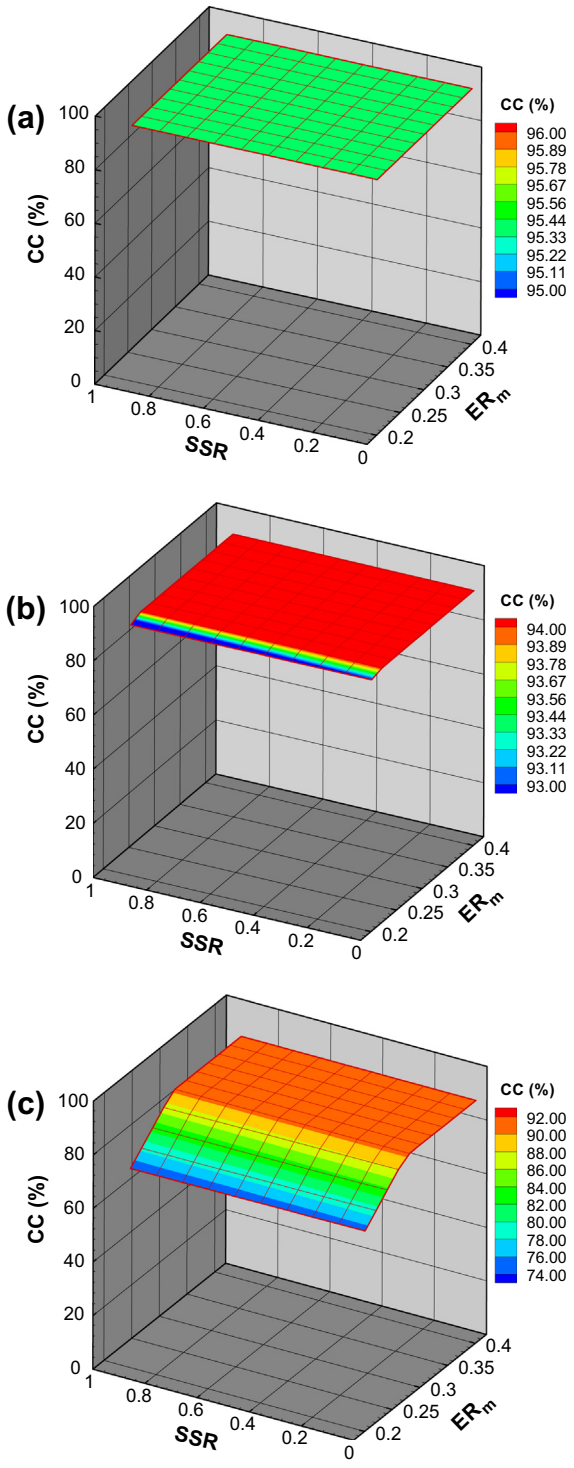

Fig. 9. Three-dimensional distributions of carbon conversion from the gasification of (a) raw bamboo, (b) torrefied bamboo at 250 °C and (c) torrefied bamboo at 300 °C.

steam flow rates at the combinations of ER_m = 0.2, 0.3, and 0.4 and SSR = 0, 0.5, and 0.9 are listed in Table 6. Fig. 6 depicts that increasing SSR facilitates the syngas yield, no matter which fuel is fed. This is a consequence of more hydrogen produced from both the water gas and shift reactions, as expressed in Eqs. (22) and (24). With the addition of steam (i.e. SSR > 0), the distributions of syngas yield of the three feedstocks are similar to those at SSR = 0, but the influence of ER_m on the variation of syngas yield diminishes. An

Table 6
A list of air and steam flow rates at various operating conditions.

Fuels	ER_m	SSR	Air (kg h^{-1})	Steam (kg h^{-1})
Raw bamboo	0.2	0	27.83	0
		0.5	14.89	3.88
		0.9	2.78	6.53
TB250		0	29.16	0
		0.5	14.58	3.80
		0.9	2.92	6.85
TB300		0	29.78	0
		0.5	13.91	3.63
		0.9	2.98	6.99
Raw bamboo	0.3	0	41.74	0
		0.5	20.87	5.44
		0.9	4.17	9.80
TB250		0	43.74	0
		0.5	21.87	5.70
		0.9	4.37	10.27
TB300		0	44.66	0
		0.5	22.33	5.82
		0.9	4.47	10.48
Raw bamboo	0.4	0	55.65	0
		0.5	27.83	7.26
		0.9	5.57	13.06
TB250		0	58.33	0
		0.5	29.16	7.61
		0.9	5.83	13.69
TB300		0	59.55	0
		0.5	29.78	7.77
		0.9	5.96	13.98

optimum ER_m can always be found at a given SSR under the situation of TB300 as the feedstock (Fig. 6c). For example, when SSR is equal to 0.9, the maximum syngas yield is 2.70 Nm^3 kg $fuel^{-1}$ which occurs at ER_m = 0.3. As far as the LHV of product gas is concerned, Fig. 7 indicates that the LHV has a drastic trend to grow when ER_m goes down and SSR goes up. The maximum values of LHV from the gasification of raw bamboo, TB250, and TB300 are located at the same place of ER_m = 0.2 and SSR = 0.9 where their values are 10.85 (Fig. 7a), 11.21 (Fig. 7b), and 11.10 MJ Nm^{-3} (Fig. 7c), respectively.

An examination of the CGE of the three fuels, Fig. 8 reveals that the distributions of CGE are consistent with those of syngas formation (Fig. 6), reflecting that the increase in CGE is due to the increase of syngas yield. When more steam is blown into the gasification system to replace air, more hydrogen will be produced from the water gas reaction and the shift reaction. This is responsible for the improvement of syngas formation. The maximum values of syngas yield and CGE of raw bamboo, TB250, and TB300 are located at (ER_m, SSR) = (0.2, 0.9), (0.22, 0.9), and (0.28, 0.9), respectively. With the condition of fixed gasification temperature (i.e. 900 °C), it is noteworthy that CGE will exceed 100% at certain operating conditions. For instance, the maximum CGE of TB250 is 119.52% which develops at ER_m = 0.22 and SSR = 0.9. Similar results have been observed in the study of Renganathan et al. [36]. It was reported that the carbon would react with CO_2 to form CO in syngas. This contributed the LHV of the syngas and caused the value of CGE being greater than 100%. In the experimental study of Nipattummakul et al. [37], they also pointed out that the value of CGE exceeding 100% from the steam gasification of wastewater sludge was a result of substantial production of syngas.

Upon inspection of the CC distribution of raw bamboo, Fig. 9a reveals that the distribution almost keeps a constant (CC = 95.4%), even though the concentrations of CO and CO_2 vary with altering ER_m and SSR (Table 4 and Fig. 6). Similar results were also observed in the study of Campoy et al., [38]. The CC of TB250 is influenced by ER_m a bit when it is less than 0.22, whereas the variation of SSR almost plays no part in CC. The maximum and

minimum values of CC from the gasification of TB250 are 94.0 and 92.3%, respectively. For TB300, its CC is also insensitive to SSR, but ER_m has a significant effect on CC in that the value changes from 74.3% to 90.6% when ER_m rises from 0.2 to 0.28. Once ER_m is larger than 0.28, the CC of TB300 remains invariant. Accordingly, it is concluded that the value of CC is mainly determined by CO and CO_2 concentrations. However, its relationship to syngas yield and CGE is slight.

4. Conclusion

A thermodynamic investigation on the gasification performances of raw bamboo, torrefied bamboo 250 °C (TB250), and torrefied bamboo at 300 °C (TB300) in a downdraft fixed bed gasifier has been carried out using Aspen Plus. From the viewpoint of syngas formation, the higher the torrefaction temperature, the better the syngas yield. However, the higher heating value of TB300 is much higher than those of raw bamboo and TB250; this results in the lowest CGE of TB300 among the three fuels. For raw bamboo and TB250, decreasing modified equivalence ratio (ER_m) and increasing steam supply ratio (SSR), corresponding to increasing CO and H_2, are able to intensify syngas formation. As a result, the CGE is enhanced and it may exceed 100% at certain operating conditions. There exists an optimum ER_m for syngas production and CGE when TB300 is gasified at a given SSR, as a consequence of much higher carbon contained in the fuel. The highest carbon content in TB300 also leads to the lowest CC among the three fuels. When simultaneously considering syngas yield, CGE, and CC, the present study indicates that TB250 is more feasible than the other two fuels for biomass gasification. However, the process of biomass torrefaction implies that extra equipment and operating costs, such as energy for biomass torrefaction, torrefied biomass cooling, and tars production, are required. On the other hand, only two torrefied biomass materials (i.e. TB250 and TB300) are considered due to limited experimental data. The topics of simultaneously considering capital and operating costs for biomass torrefaction and gasification as well as the optimum torrefaction temperature deserve further investigation in the future.

Acknowledgment

The authors gratefully acknowledge the financial support of the National Science Council, Taiwan, ROC, on this study.

References

[1] Bi XT, Liu X. High density and high solids flux CFB risers for steam gasification of solids fuels. Fuel Process Technol 2010;91:915–20.
[2] Chen WH, Chen JC, Tsai CD, Jiang TL. Transient gasification and syngas formation for coal particles in a fixed-bed reactor. Int J Energ Res 2007;31:895–911.
[3] Chen WH. A simplified model of predicting coal gasification performance in a partial oxidation environment. Int Commun Heat Mass 2007;34:623–9.
[4] Chmielniak T, Sciazko M. Co-gasification of biomass and coal for methanol synthesis. Appl Energ 2003;74:393–403.
[5] Bludowsky T, Agar DW. Thermally integrated bio-syngas-production for biorefineries. Chem Eng Res Des 2009;87:1328–39.
[6] Chen WH, Lin BJ, Lee HM, Huang MH. One-step synthesis of dimethyl ether from the gas mixture containing CO_2 with high space velocity. Appl Energ 2012;98:92–101.
[7] Buragohain B, Mahanta P, Moholkar VS. Biomass gasification for decentralized power generation: the Indian perspective. Renew Sust Energ Rev 2010;14:73–92.
[8] Sheth PN, Babu BV. Experimental studies on producer gas generation from wood waste in a downdraft biomass gasifier. Bioresource Technol 2009;100:3127–33.
[9] Lv P, Yuan Z, Ma L, Wu C, Chen Y, Zhu J. Hydrogen-rich gas production from biomass air and oxygen/steam gasification in a downdraft gasifier. Renew Energ 2007;32:2173–85.
[10] Gonzáleza JF, Romána S, Bragadoa D, Calderónb M. Investigation on the reactions influencing biomass air and air/steam gasification for hydrogen production. Fuel Process Technol 2008;89:764–72.
[11] Gai C, Dong Y. Experimental study on non-woody biomass gasification in a downdraft gasifier. Int J Hydrogen Energ 2012;37:4935–44.
[12] Gordillo G, Annamalai K, Carlin N. Adiabatic fixed-bed gasification of coal, dairy biomass, and feedlot biomass using an air–steam mixture as an oxidizing agent. Renew Energ 2009;34:2789–97.
[13] Lv PM, Xiong ZH, Chang J, Wu CZ, Chen Y, Zhu JX. An experimental study on biomass air–steam gasification in a fluidized bed. Bioresource Technol 2004;95:95–101.
[14] Puig-Arnavat M, Bruno JC, Alberto C. Review and analysis of biomass gasification models. Renew Sust Energ Rev 2010;14:2841–51.
[15] Li X, Grace JR, Watkinson AP, Lim CJ, Ergudenler A. Equilibrium modeling of gasification: a free energy minimization approach and its application to a circulating fluidized bed coal gasifier. Fuel 2001;80:195–207.
[16] Jarungthammachote S, Dutta A. Equilibrium modeling of gasification: Gibbs free energy minimization approach and its application to spouted bed and spout-fluid bed gasifiers. Energ Convers Manage 2008;49:1345–56.
[17] Nikoo MB, Mahinpey N. Simulation of biomass gasification in fluidized bed reactor using Aspen Plus. Biomass Bioenerg 2008;32:1245–54.
[18] Doherty W, Reynolds A, Kennedy D. The effect of air preheating in a biomass CFB gasifier using Aspen Plus simulation. Biomass Bioenerg 2009;33:1158–67.
[19] Ramzan N, Ashraf A, Naveed S, Malik A. Simulation of hybrid biomass gasification using Aspen Plus: a comparative performance analysis for food, municipal solid and poultry waste. Biomass Bioenerg 2011;35:3962–9.
[20] Lu KM, Lee WJ, Chen WH, Liu SH, Lin TC. Torrefaction and low temperature carbonization of oil palm fiber and eucalyptus in nitrogen and air atmospheres. Bioresource Technol 2012;123:98–105.
[21] Chen WH, Kuo PC. A study on torrefaction of various biomass materials and its impact on lignocellulosic structure simulated by a thermogravimetry. Energy 2010;35:2580–6.
[22] Li H, Liu X, Legros R, Bi XT, Lim CJ, Sokhansanj S. Torrefaction of sawdust in a fluidized bed reactor. Bioresource Technol 2012;103:453–8.
[23] Chew JJ, Doshi V. Recent advances in biomass pretreatment – torrefaction fundamentals and technology. Renew Sust Energ Rev 2011;15:4212–22.
[24] van der Stelet MJC, Gerhauser H, Kiel JHA, Ptasinski KJ. Biomass upgrading by torrefaction for the production of biofuels: a review. Biomass Bioenerg 2011;35:3748–62.
[25] Chen WH, Cheng WY, Lu KM, Huang YP. An evaluation on improvement of pulverized biomass property for solid fuel through torrefaction. Appl Energ 2011;88:3636–44.
[26] Prins MJ, Ptasinski KJ, Janssen FJJG. More efficient biomass gasification via torrefaction. Energy 2006;31:3458–70.
[27] Deng J, Wang GJ, Kuang JH, Zhang YL, Luo YH. Pretreatment of agricultural residues for co-gasification via torrefaction. J Anal Appl Pyrol 2009;86:331–7.
[28] Couhert C, Salvador S, Commandre JM. Impact of torrefaction on syngas production from wood. Fuel 2009;88:2286–90.
[29] Smith JM, Van Ness HC, Abbott MM. Introduction to Chemical Engineering Thermodynamics. 7th ed. New York: McGraw-Hill; 2005.
[30] Koukkari P, Pajarre R. Introducing mechanistic kinetics to the Lagrangian Gibbs energy calculation. Comput Chem Eng 2006;30:1189–96.
[31] Chen WH, Lin MR, Jiang TL, Chen MH. Modeling and simulation of hydrogen generation from high temperature and low-temperature water gas shift reactions. Int J Hydrogen Energ 2008;33:6644–56.
[32] Jayah TH, Aye L, Fuller RJ, Stewart DF. Computer simulation of a downdraft wood gasifier for tea drying. Biomass Bioenerg 2003;25:459–69.
[33] Jarungthammachote S, Dutta A. Thermodynamic equilibrium model and second law analysis of a downdraft waste gasifier. Energy 2007;32:1660–9.
[34] Baratieri M, Baggio P, Fiori L, Grigiante M. Biomass as an energy source: thermodynamic constraints on the performance of the conversion process. Bioresource Technol 2008;99:7063–73.
[35] Chen WH, Du SW, Tsai CH, Wang ZY. Torrefied biomasses in a drop tube furnace to evaluate their utility in blast furnaces. Bioresource Technol 2012;111:433–8.
[36] Renganathana T, Yadava MV, Pushpavanama S, Voolapallib RK, Choc YS. CO_2 utilization for gasification of carbonaceous feedstocks: a thermodynamic analysis. Chem Eng Sci 2012;83:159–70.
[37] Nipattummakul N, Ahmed I, Kerdsuwan S, Gupta AK. High temperature steam gasification of wastewater sludge. Appl Energ 2010;87:3729–34.
[38] Campoy M, Gómez-Barea A, Vidal FB, Ollero P. Air–steam gasification of biomass in a fluidised bed: process optimisation by enriched air. Fuel Process Technol 2009;90:677–85.